The conduit system exports locally secreted IgM from lymph nodes

Guilhem R. Thierry[1], Mirela Kuka[2] ⓘ, Marco De Giovanni[2] ⓘ, Isabelle Mondor[1], Nicolas Brouilly[3], Matteo Iannacone[2]* ⓘ, and Marc Bajénoff[1]* ⓘ

Immunoglobulin M (IgM) is the first type of antibody produced during acute infections and thus provides an early line of specific defense against pathogens. Being produced in secondary lymphoid organs, IgM must rapidly be exported to the blood circulation. However, it is currently unknown how such large pentameric molecules are released from lymph nodes (LNs). Here, we show that upon immunization, IgM transiently gains access to the luminal side of the conduit system, a reticular infrastructure enabling fast delivery of tissue-derived soluble substances to the LN parenchyma. Using microinjections of purified IgM, we demonstrate that conduit-associated IgM is delivered by neither the afferent lymph nor the blood, but is locally conveyed by conduits. Exploiting in vivo models, we further demonstrate that conduit-associated IgM is locally and transiently produced by activated, antigen-specific B cells migrating in the T cell zone. Thus, our study reveals that the conduit system is coopted by B cells to rapidly export secreted IgM out of LNs.

Introduction

It is widely accepted that IgM provides a first line of defense during viral, bacterial, and parasitic infections, before the generation of high-affinity IgG responses that are important for long-lived immunity and immunological memory (Baumgarth et al., 2000; Diamond et al., 2003; Salinas-Carmona and Pérez-Rivera, 2004; Couper et al., 2005; Racine and Winslow, 2009). Antigen (Ag)-specific IgM is secreted by plasmablasts in secondary lymphoid organs and can be detected in the efferent lymph, leaving reactive LNs as soon as 4 d following immunization (Cahill et al., 1974; Gohin et al., 1997; Haig et al., 1999). At that time, B cells recruited into extrafollicular responses are still located in the T cell zone and the medullary cords (Luther et al., 1997a,b). Since they weigh ∼1,000 kD and are assembled in pentamers, IgM molecules should poorly diffuse in the LN parenchyma. This apparent discrepancy raises the question of how such large molecules are rapidly exported out of reactive LNs.

The LN is equipped with a three-dimensional (3D) meshwork of reticular fibers known as the conduit system (Anderson and Anderson, 1975; Sainte-Marie and Peng, 1986; Gretz et al., 1996), an infrastructure that emerges from the subcapsular sinus (SCS) and extends throughout the parenchyma. This system allows the fast delivery of lymph-borne soluble substances such as cytokines (Gretz et al., 2000) and Ag (Sixt et al., 2005) from the SCS to the T cell zone. Conduits, therefore, constantly proj-

ect the immune status of peripheral tissues to their most proximal draining LNs (dLNs). Once they have entered the conduits, lymph-borne molecules migrate unidirectionally from the SCS to the deep parenchyma, where they are eventually discharged into high endothelial venules (HEVs) and the medullary sinus (Gretz et al., 2000). In the SCS, sinus-lining cells act as a molecular sieve for lymph-borne molecules, preventing large components weighing more than 70 kD from entering the conduits (Gretz et al., 2000; Rantakari et al., 2015). Thus, any lymph-borne molecule exceeding 70 kD cannot access the conduit system and remains in the SCS.

Here, we have explored cellular and structural mechanisms that control the transport of IgM within the LN parenchyma. We show that soluble IgM transiently locates within the conduit system in immunized LNs, despite its size. We further demonstrate that conduit-associated IgM originates from neither the lymph nor the blood of immunized mice and that IgM injected directly into the LN parenchyma accesses and is conveyed by the conduit system. Finally, we designed different mouse models to track Ag-specific IgM produced in reactive LNs and confirmed that the conduit system physiologically transports IgM secreted in the LN parenchyma during an immune response. Collectively, our results reveal that B cells use the conduit system to rapidly export the first wave of protective Ig to the periphery.

Results and discussion

IgM localizes within the conduit system of reactive LNs

After being secreted by plasmablasts located in the T cell area and the medulla of reactive LNs, IgM reaches the efferent lymph and eventually the blood circulation. Previous experiments performed in sheep demonstrated that Ag-specific IgM can be measured in the efferent lymph of reactive LNs a few days following infection (Gohin et al., 1997). How IgM secreted in the interstitial milieu of the LN reaches the efferent lymphatic vessel and the blood circulation is presently unknown. We hypothesized that free dispersion of such large molecules would represent an inefficient way to rapidly export IgM. To locate any structural infrastructure devoted to this purpose, we first immunized WT (C57BL/6J) and B cell–deficient (J$_H$T; Gu et al., 1993) mice with CFA and performed immunostainings at the peak of the IgM response. As expected, IgM signal was absent from the LNs of B cell–deficient mice and colocalized with follicular B cells in control and reactive LNs of WT mice (Fig. 1 A). In reactive WT LNs, a second reticular pattern of IgM signal was observed in the T cell zone. As this area is supported by a 3D meshwork of reticular fibers known as the conduit system, we stained LN sections for collagen IV expression, an extracellular matrix molecule abundantly present in this infrastructure (Sixt et al., 2005). Data shown in Fig. 1 A indicate that IgM and collagen IV signals indeed colocalized. To determine whether IgM was positioned in the luminal side of the conduits, where the lymph circulates, or adsorbed on the surface of the fibroblastic reticular cells (FRCs) that enwrap the conduits, we took advantage of *Ccl19*-Cre:Rosa^{tdT} mice in which FRCs are fluorescent (Chai et al., 2013). Immunostaining of reactive LNs harvested from these mice revealed that IgM was not adsorbed on FRCs but located in the lumen of the collagen IV–expressing conduits (Fig. 1 B), a result that we further confirmed by electron microscopy (EM; Fig. 1 C). Taken together, these findings indicate that despite its large size and pentameric assembly, IgM can access the conduit system of reactive LNs.

Conduit-associated IgM originates from neither the lymph nor the blood

IgM found in the conduit system could have three origins. Tissue inflammation induces local vascular permeability and leakage of large plasma molecules (Ono et al., 2017). Therefore, serum IgM might have been drained to the proximal LN via the lymph. Additionally, LN blood vessels such as HEVs and the primary feeding arteriole are highly sensitive to tissue-derived inflammatory signals (Soderberg et al., 2005; Mondor et al., 2016; Ager, 2017). Thus, increased permeability of these vessels might allow IgM access to the conduits. Finally, plasmablasts undergoing proliferation in the T cell zone and medullary cords might have locally produced the IgM (MacLennan et al., 2003). When injected in the skin, molecules weighing >70 kD are transported via the lymph to the proximal dLN and discharged in its SCS, but are unable to enter the underlying conduit system (Fig. S1 A; Gretz et al., 2000). This limitation is imposed by a filtration system controlled by the plasmalemma vesicle–associated protein, an endothelial protein produced by the sinus-lining cells (Rantakari et al., 2015). In agreement with this, we observed that IgM injected s.c. in the ears of control or CFA-preimmunized J$_H$T mice was un-

able to cross the SCS, whereas a coinjected, smaller fluorescent tracer, wheat germ agglutinin (WGA; 38 kD), was readily able to enter the conduit system (Fig. 2 A). SCS macrophages reside in the SCS and are known to transfer lymph-borne Ag and immune complexes to follicular B cells (Carrasco and Batista, 2007; Junt et al., 2007; Phan et al., 2007). Because SCS macrophages are reduced in the absence of B cells (Phan et al., 2009; Moseman et al., 2012), we reasoned that the inability of IgM to cross the SCS of J$_H$T mice might result from the lack of SCS macrophages. To test this hypothesis, we took advantage of D$_H$LMP2A mice (Casola et al., 2004), in which the J$_H$ segment of the IgH locus is replaced by the EBV-derived LMP2A protein that functions as a surrogate survival signal for B cells. Therefore, D$_H$LMP2A mice retain B cells, SCS macrophages, and normal lymphoid tissue architecture but are devoid of surface-expressed and secreted Ig (Moseman et al., 2012). Subcutaneous delivery of purified IgM and WGA to D$_H$LMP2A mice yielded identical results as in J$_H$T mice (Fig. S1, B and C), indicating that conduit-associated IgM could not have been carried by the afferent lymph. The absence of IgM in the conduits of nondraining LNs (ndLNs) of CFA-immunized mice (Fig. 1 B) suggested that conduit-associated IgM does not originate from the blood either. To formally exclude this possibility in reactive LNs, whose vasculature might be more permeable than at steady state, we injected the serum of CFA-preimmunized WT mice in the bloodstream of CFA-immunized J$_H$T and D$_H$LMP2A mice together with fluorescent WGA. Although IgM and WGA were both found in the SCS and large blood vessels of enlarged LNs, only WGA reached the conduit system, ruling out a blood origin for conduit-associated IgM (Figs. 2 B and S1 D).

The conduit system transports large molecules delivered in the parenchyma

We hypothesized that conduit-associated IgM observed in reactive LNs is produced locally by plasmablasts. As a first attempt to test this assumption, we compared the ability of IgM and WGA to diffuse via the conduit system upon direct delivery into the LN parenchyma. To this end, commercially available, purified IgM and fluorescent WGA were coinjected directly into the enlarged dLNs of J$_H$T mice immunized with CFA 10 d before. As expected based on its small molecular weight, WGA diffused in the numerous ramifications of the conduit system (Fig. 3 A). Despite its size, IgM also displayed a similar pattern of diffusion, suggesting that IgM secreted in the parenchyma could also access and be conveyed by the conduit system. Microinjections of fresh serum from immunized WT mice in reactive inguinal LNs of J$_H$T mice yielded the same results (data not shown). We then tested the specificity of IgM uptake by injecting a fluorescent dextran weighing 150 kD. As indicated in Fig. 3 B, this large dextran that was unable to reach the conduit system when injected s.c. (Fig. S1 A) was efficiently transported to the conduits upon intranodal delivery. Additionally, similar results were obtained in D$_H$LMP2A mice (Fig. S2, A and B). To exclude the possibility that the fixation protocol cross-linked proteins, including IgM, in the conduit lumen in an unspecific manner, we conjugated purified IgM molecules to fluorescent probes and injected them in combination with labeled WGA into the reactive LNs of WT mice (Fig. S2, C and D). Fresh, unfixed LNs were then sectioned using
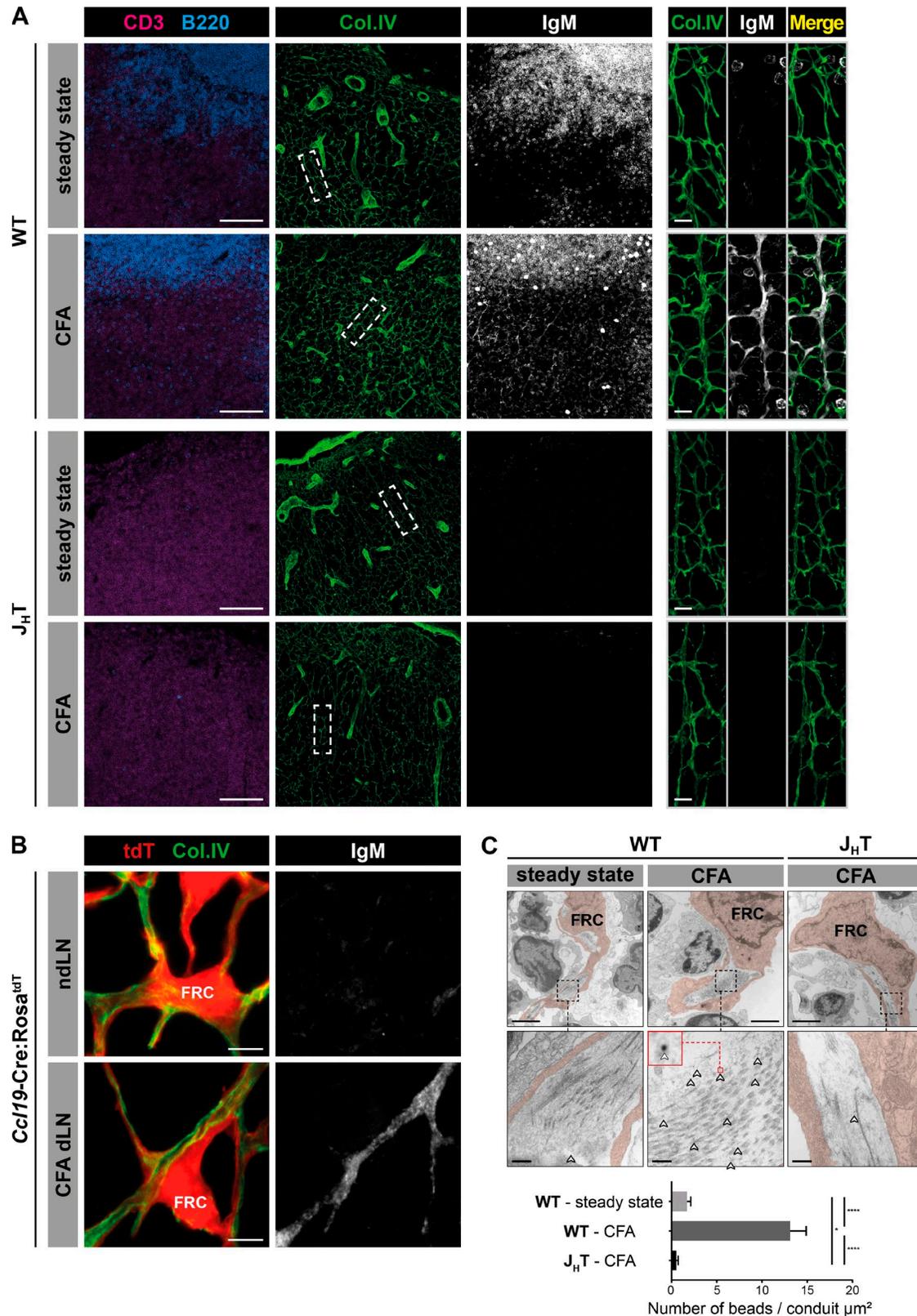
Figure 1.   **IgM localizes within the conduit system of reactive LNs. (A)** Confocal imaging of reactive and steady state auricular LNs from WT (C57BL/6J) or B cell–deficient (J$_H$T) mice, 10 d after intradermal CFA immunization in the ears. Sections were stained for CD3, B220, collagen IV (col.IV), and IgM. Insets display high-magnification views of collagen IV$^+$ conduits in the T cell zone. Bars, 100 µm (left panels); 10 µm (right panels). Data are representative of three experiments (two mice per condition and experiment). **(B)** Confocal imaging of auricular dLNs and contralateral ndLNs from *Ccl19*-Cre:Rosa^{tdT} mice, 10 d after intradermal CFA injection in one ear. Sections were stained for collagen IV and IgM. tdT, tdTomato. Bars, 5 µm. Pictures are representative of three experiments (two mice per experiment). **(C)** Representative EM pictures of FRCs and conduits in steady state and auricular reactive LNs of WT and J$_H$T mice, 10 d after intradermal

a vibratome and immediately imaged by confocal microscopy. Using this approach, fluorescent IgM and WGA distributed into the conduit system, just as in fixed sections.

Finally, in order to estimate the speed and directionality of molecules transported by the conduit system, which should approximately reflect the transport rate of IgM molecules, we performed s.c. injections of fluorescent WGA in immunized WT mice and compared the distribution at different time points (Fig. S2, E and F). Within a minute, the fluorescent tracer reached the SCS and the follicular conduits. 4 min later, it propagated from B cell follicles to the T cell zone conduits, ∼150 µm deeper in the parenchyma, at a speed of ∼35 µm/min. Therefore, small and large molecules present in the LN parenchyma have access to and are rapidly transported by the conduit system in a nonspecific manner from the SCS to the deep parenchyma.

The conduit system transports locally secreted IgM during an immune response

Intranodal injection might alter the stromal network and interfere with the physiological flow of lymph in the parenchyma. This raises the question of whether paracortical IgM also enters the conduit system under physiological conditions. To track Ag-specific IgM normally produced during an immune response, we designed two sets of experiments. In the first one, we used MD4 mice in which all B cells express a BCR specific for hen egg lysozyme (HEL; Goodnow et al., 1988). As the MD4 BCR was originally cloned in a Balb/c strain, C57BL/6 MD4 B cells still carry the "a" allotype of IgM (IgM_a) expressed in Balb/c, whereas the polyclonal B cells of a C57BL/6 WT mouse carry the "b" allotype of IgM (IgM_b). Taking advantage of this allotypic difference, we adoptively cotransferred C57BL/6 mice with MD4 B cells and OVA-specific OT-II CD4^{+} T helper cells (Barnden et al., 1998). Recipient mice were then immunized with an emulsion of CFA containing an HEL-OVA chimeric protein. This protocol induced robust extrafollicular proliferation of MD4 B cells (Garside et al., 1998) and a concomitant HEL-specific IgM_a response as early as 4 d later (Fig. 4). Although IgM_a was detected on the surface of adoptively transferred MD4 cells in ndLNs and dLNs, an additional reticular signal appeared in dLNs when extrafollicular MD4 B cells were relocated to the T cell zone. Data shown in Fig. 4 A indicate that IgM_a colocalized with collagen IV[+] conduits. We then performed similar experiments in *Ccl19*-Cre:Rosa[tdT] mice harboring fluorescent FRCs and confirmed that soluble IgM_a was in the luminal side of conduits, supporting the ability of this system to channel locally secreted IgM also during an immune response (Fig. 4 B).

In the second experimental model, we analyzed the ability of the conduit system to transport IgM upon viral infection. Vesicular stomatitis virus (VSV) is a cytopathic virus that is rapidly controlled by a strong, early, initially T cell–independent neutralizing IgM response that switches to a T cell–dependent IgG response after 4–6 d (Ochsenbein et al., 2000). We took advantage of VSV-specific BCR transgenic mice (referred to as VI10YEN;

Hangartner et al., 2003) to track VSV-specific IgM in situ (Fig. 5). VI10YEN B cells were adoptively transferred into Ig-deficient D_HLMP2A mice. In this experimental setting, IgM can originate only from the activated VI10YEN B cells and hence is specific for VSV. Recipient mice were infected s.c. with VSV, and their reactive LNs were analyzed 4 and 7 d later by imaging (Fig. 5). As expected, no IgM signal was detected in LNs from mice that did not receive VI10YEN B cells, even after VSV infection (Fig. 5, upper panels). In mice that were transferred with VI10YEN B cells, but not infected with VSV, IgM signal was exclusively detected on the surface of VSV-specific B cells (Fig. 5, lower panels). Upon VSV infection, VI10YEN B cells massively proliferated and relocated to the T/B interface at day 4, a time when they are known to secrete abundant levels of soluble IgM (Ochsenbein et al., 1999; Hangartner et al., 2003). Closer examination indicated that these IgM molecules were associated with the conduit system (Fig. 5, lower panels). This association was transient, as conduit-associated IgM disappeared from the dLNs at day 7, suggesting that the early protective wave of neutralizing IgM was already exported from the LNs at that time. Interestingly, 4 d after infection, IgM also associated with peripheral node addressin (PNAd)–expressing HEVs and Lyve1-expressing lymphatic endothelial cells of cortical and medullary sinusoids in LNs (Fig. S3 A). Because these vascular structures show connectivity and continuity with the conduit system (Anderson and Anderson, 1975; Huang et al., 2018; Fig. S3, B and C), HEVs and lymphatic sinusoids could both represent an exit route for IgM from LNs. The relative importance of these two exit routes remains to be determined.

Collectively, these results indicate that IgM produced during an early antiviral response is also channeled by the conduit system to be rapidly exported from the LN.

Concluding remarks

The first wave of neutralizing IgM produced in LNs must rapidly gain access to the periphery to exert its protective functions. Considering the large size and the multimerization of IgM, we reasoned that passive diffusion of such molecules from the LN parenchyma to the efferent lymphatics would hamper the efficiency of this process. Here, we provide an alternative scenario by showing that the export of IgM from the LN relies on the conduit system, a 3D meshwork of reticular fibers devoted to the fast transport of lymph-borne molecules throughout the LN paracortex.

Conduits are formed by multiple, concentric layers of various extracellular matrix molecules ensheathed by a cellular rim of FRC (Sixt et al., 2005). This system is thought to be sealed in order to (a) prevent spread of lymph-borne Ag to the LN cortex and (b) ensure fast delivery of inflammatory soluble mediators to HEVs (Gretz et al., 2000). However, Sixt et al. (2005) suggested that dendritic cells associated with the reticular fibers can sample the content of the conduit system, whereas an EM study revealed that ∼10% of the conduit system is not actually

---

CFA injection in one ear. Ultrathin sections were stained with 6-nm gold nanobeads specific for mouse IgM (highlighted with arrowheads), and the average number of beads located in the conduit lumen was evaluated for each condition. Bars, 2 µm (upper panels); 200 nm (lower panels). Data are representative of two experiments (one individual per condition and experiment). Results are expressed as mean ± SEM. *, P < 0.05; ****, P < 0.0001.
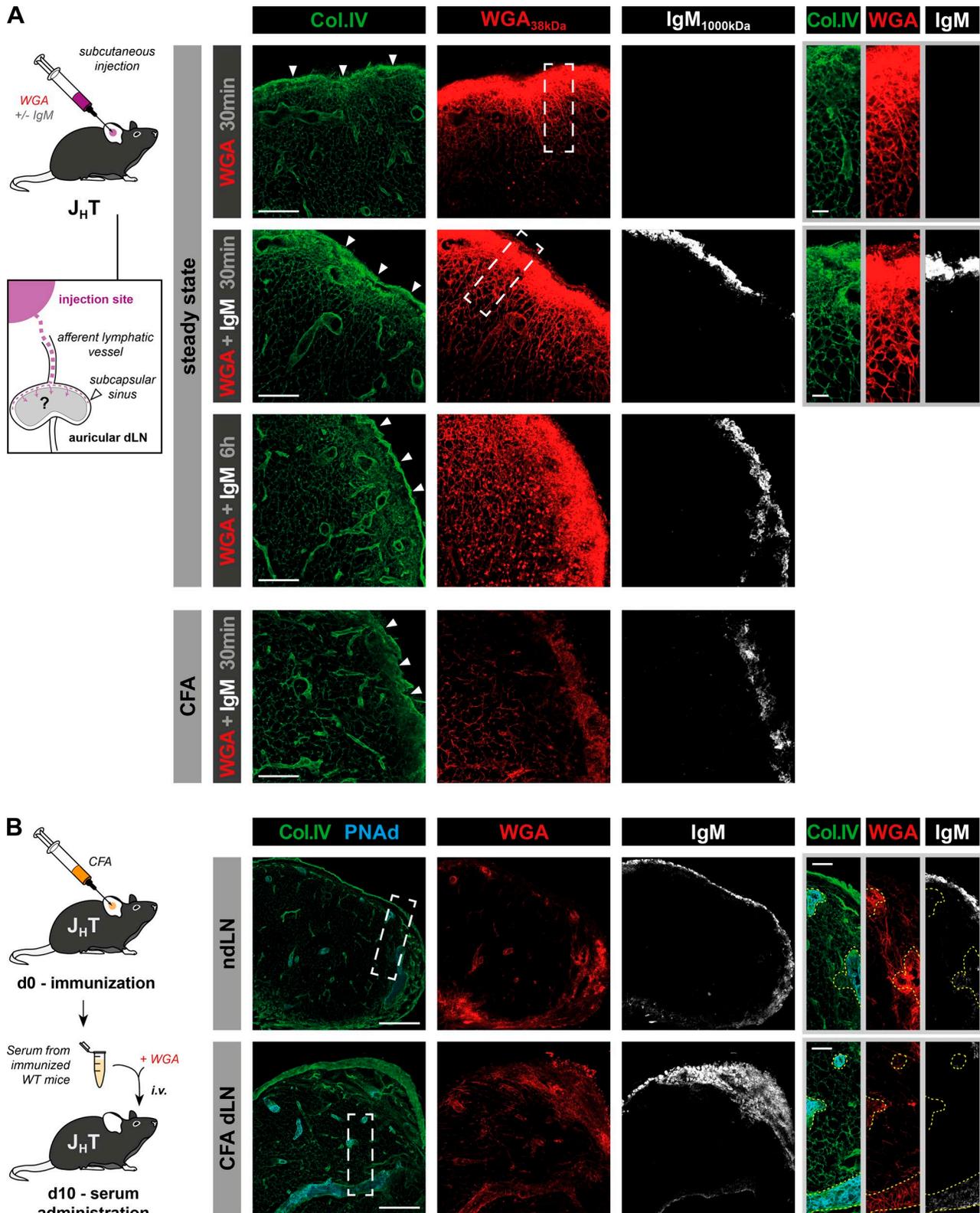
Figure 2. **Lymph- and blood-borne soluble IgM does not access the conduit system. (A)** Unimmunized J_HT mice or animals that received an intradermal injection of CFA 10 d before in one ear were injected s.c. with fluorescent WGA ($\sim$38 kD) with or without purified mouse IgM ($\sim$1,000 kD) and their auricular dLNs were harvested at the indicated time points. LN sections were stained for collagen IV (Col.IV) and IgM. Arrowheads indicate SCS. Insets show high-magnification views of the SCS and the underlying cortex. Bars, 100 µm (left panels); 20 µm (right panels). Data are representative of three experiments (two mice per condition and experiment). **(B)** J_HT and WT mice were injected intradermally with CFA in one ear. 10 d later, J_HT mice were supplemented with the serum

covered by FRCs (Hayakawa et al., 1988). Therefore, it is possible that the conduit system possesses discrete physical access points for parenchymal molecules (Ushiki et al., 1995). As plasmablasts tend to migrate randomly with long free paths in the LN parenchyma before reaching the medullary cords (Fooksman et al., 2010), they might use the FRC network as a migration scaffold and release their IgM in these putative access points. This process would be consistent with the reported ability of B cells to sample lymph-borne Ag from conduits in B follicles (Roozendaal et al., 2009). The fact that inert, large molecules such as dextran can also access the conduit system when delivered intranodally suggests that the entry of IgM into the conduits does not require a dedicated system such as Fc receptors, but rather favors a model in which any soluble molecule present in the interstitial milieu of the parenchyma would be drained by this process. LNs are densely packed organs in which 95% of the cells continuously migrate (Bajénoff, 2012). We anticipate that such cellular packing and constant fluid motion would induce significantly higher pressure in the parenchyma (compared with the conduit lumen), hence enabling interstitial fluids to flow into the conduits where a lower hydrostatic pressure would exist.

Our results confirmed that the inability of lymph-borne IgM to enter the conduit system is largely dictated by the filtering system present in the sinus lining floor of the SCS (Rantakari et al., 2015) and not linked to collagen fibers and fibrils located in the conduit lumen as previously proposed (Gretz et al., 1997). We believe that this restriction represents an important aspect of the efficacy of the IgM export system. Knowing that any delay in antibody response exposes the host to pathogen dissemination and susceptibility (Kalinke et al., 1996; Lutz et al., 1998), the first wave of IgM produced in the LN should rapidly reach the infected tissue via the blood. While conduit-mediated transport of IgM within a single LN represents an efficient way to export IgM to the efferent lymphatics, this mode of transportation becomes highly effective at an organismal level in combination with the filtering system present in the SCS: LNs are associated in chains in which the efferent lymphatic content of a given LN is discharged in the SCS of the downstream LN. If IgM molecules were able to enter the conduit system of all the LNs present in the chain, their release in the thoracic duct would be dramatically slowed down. In the presence of this molecular sieve, however, IgM arriving in the SCS of every downstream LN only flows through the SCS and the medullary sinuses, which represents the fastest delivery route to the thoracic duct.

Subcutaneously injected soluble factors such as chemokines are rapidly delivered to the luminal side of the HEV via the conduit system (Anderson and Anderson, 1975; Gretz et al., 2000). This process is thought to ensure an immediate modulation of lymphocyte trafficking in inflamed LN. Moreover, experimental and computational studies have suggested that under baseline conditions, some of the fluid flows from lymphatic passageways to blood vessels in LNs (Adair and Guyton, 1983; Jafarnejad et al.,

2015). In agreement with this notion, we observed anti-VSV IgM associating with the conduits directly surrounding the HEVs of reactive LNs following VSV infection. It remains possible, therefore, that a fraction of IgM antibodies is directly released in the blood vessels of the LN via the conduits, ensuring its most rapid delivery to the infected tissue.

In summary, we studied how the first wave of Ig produced upon infection, IgM, is exported from the LN. We found that this export occurs through the conduit system and thereby identified a novel biological function for this network, underlining its importance beyond structural support.

Materials and methods

Mice

All mice were 8–12 wk of age on a C57BL/6 background. WT C57BL/6J mice were purchased from Janvier Labs. B cell–deficient J_HT mice (B6.129P2-Igh-J^{tm1Cgn}; Gu et al., 1993) and MD4 mice (B6.BALB/c-Tg(IghelMD4)4Ccg; Goodnow et al., 1988) were a gift from N. Fazilleau (Centre de Physiopathologie de Toulouse Purpan, INSERM U1043, CNRS UMR5282, Université Toulouse III Paul-Sabatier, Toulouse, France). Prox1-CreER^{T2} mice (B6.129S1-Prox1$^{tm3(cre/ERT2)Gco}$; Bazigou et al., 2011) were a gift from T. Makinen (Department of Immunology, Genetics and Pathology, Uppsala University, Uppsala, Sweden). Ccl19-Cre mice (C57BL/6N-Tg(Ccl19-cre)489Biat; Chai et al., 2013) were purchased from the European Mouse Mutant Archive (INFRAFRON TIER). Rosa^{tdT} mice (B6.Cg-Gt(ROSA)26Sor$^{tm14(CAG-tdTomato)Hze}$, also known as Ai14; Madisen et al., 2010) were obtained from JAX. OT-II mice (B6.129S6-Tg(TcraTcrb)425Cbn; Barnden et al., 1998) were purchased from Taconic Biosciences. D_HLMP2A mice (B6.BALB/c-Igh$^{tm5.1Cgn}$; Casola et al., 2004), backcrossed for >10 generations against C57BL/6 mice, were provided by M. Iannacone (Milan, Italy). Heavy-chain knock-in and light-chain BCR transgenic mice specific for VSV Indiana (VI10YEN; B6.Cg-Igh-J$^{tm1(VDJ-VI10)Zbz}$; Hangartner et al., 2003) were obtained through the European Virus Archive. Mice were bred and maintained under specific pathogen–free conditions at the Centre d'Immunologie de Marseille Luminy (Marseille, France). Mice were housed under a standard 12-h/12-h light–dark cycle with food and water ad libitum. Age- and sex-matched littermate mice were used. Experimental procedures were conducted in accordance with French and European guidelines for animal care under the permission number 5-01022012 following review and approval by the local animal ethics committee in Marseille. Experiments involving the D_HLMP2A and VI10YEN strains were performed at the San Raffaele Scientific Institute (Milan, Italy) following approval by the local ethics committee.

Antibodies and specific reagents

For immunostaining and confocal imaging, purified anti–collagen IV (polyclonal rabbit IgG) was obtained from Abcam. Lyve1

---

of the immunized WT mice over a 24-h period and injected i.v. with fluorescent WGA 5 min before the harvest of reactive and contralateral auricular LNs. Data show confocal images from LN sections stained for collagen IV, PNAd, and IgM. Insets display high-magnification views of PNAd$^+$ HEVs (yellow dashed line) and surrounding conduits. Bars, 200 µm (left panels); 50 µm (right panels). Data are representative of two experiments (three mice per experiment).
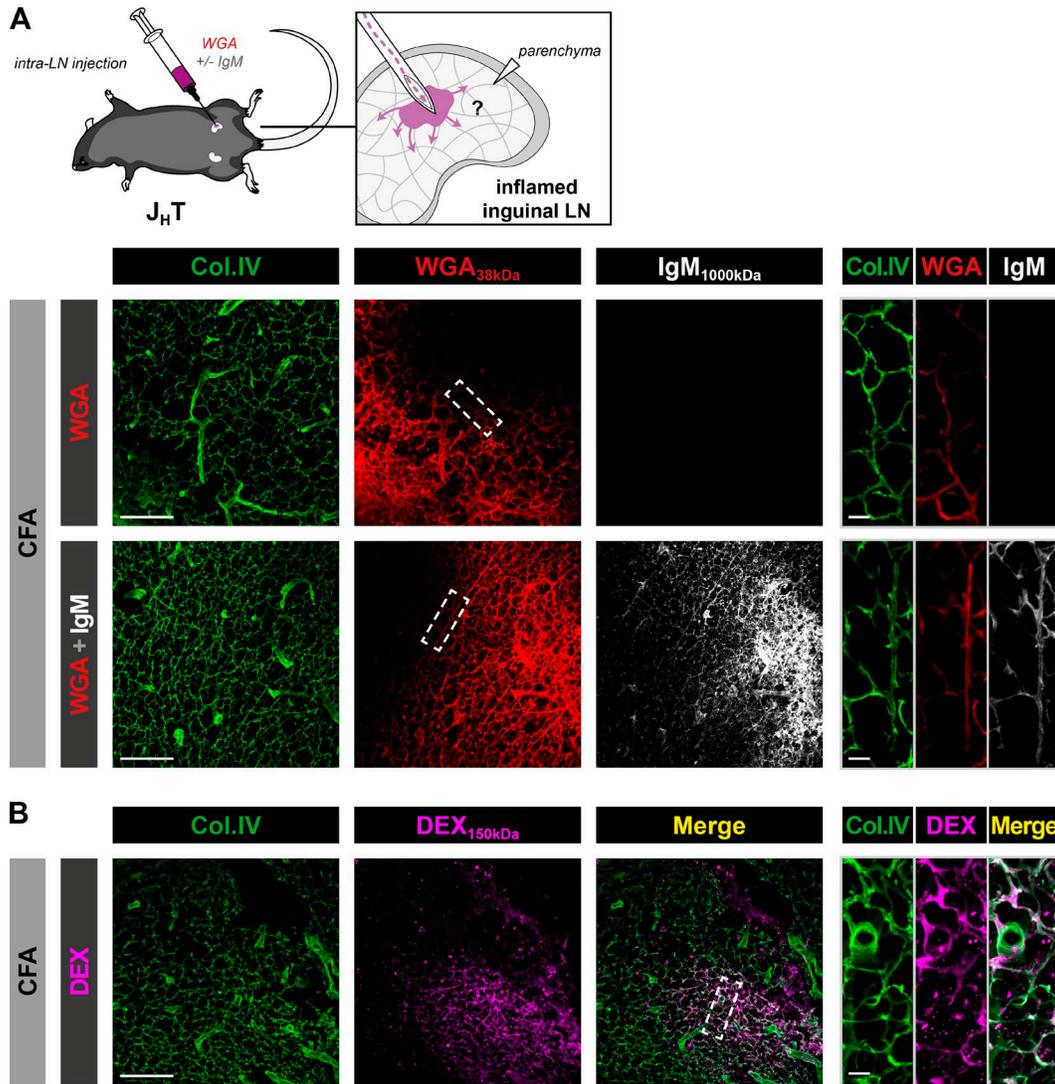
Figure 3. The conduit system transports soluble IgM upon intranodal injection. (A and B) J_HT mice were injected intradermally with CFA at the base of the tail. 10 d later, draining inguinal LNs were surgically exposed and microinjected with fluorescent WGA with or without purified mouse IgM (A) or 150-kD fluorescent dextran (DEX; B). Data show confocal images from inguinal LN sections stained for collagen IV (Col.IV) and IgM. Insets display high-magnification views of conduits from the diffusion front. Bars, 100 µm (left panels); 10 µm (right panels). Data are representative of three experiments (two mice per condition and experiment) in A and B.

monoclonal antibody (ALY7) was from eBiosciences. Antibodies directed against mouse IgM or rat IgG and rabbit IgG were purchased from Jackson ImmunoResearch and BioLegend. Specific antibodies recognizing mouse CD3 (17A2), B220 (RA3-6B2), and IgM_a (MA-69) were purchased from BioLegend and visualized by direct coupling to phycoerythrin, Pacific Blue, and FITC, respectively. For transmission EM and gold nanobead immunolabeling, goat IgG conjugated to 6-nm gold nanoparticles and directed against the µ-chain of mouse IgM was purchased from Aurion (806.033). For injection experiments, purified mouse IgM was purchased from BD PharMingen (G155-228) and Rockland Immunochemicals (010–0107). Soluble tracers such as WGA coupled to Alexa Fluor 488 (AF488) or AF555 and 10-kD dextran (Dex_{10kD}) coupled to tetramethylrhodamine (TMR) were obtained from Thermo Fisher Scientific, and 150-kD dextran (Dex_{150kD}) coupled to FITC was from Sigma-Aldrich. According

to the provider's instructions, we estimated the total molecular weight of fluorescent tracers as follows: 39–41 kD for AF488-WGA and AF555-WGA, 10–11 kD for $TMR-Dex_{10kD}$, and 151–157 kD for $FITC-Dex_{150kD}$. For injection of soluble IgM conjugated to fluorescent probe, polyclonal purified mouse IgM was labeled with AF647 *N*-hydroxysuccinimide ester from Thermo Fisher Scientific (A200006). For cell isolation and adoptive transfer, biotinylated antibodies directed against mouse CD8 (H35-17.2) and B220 (RA3-6B2) were purchased from eBioscience; biotinylated anti-CD3 (17A2) and anti-CD11b (M1/70) were from BioLegend. Anti-biotin magnetic beads were obtained from Miltenyi Biotec.

Immunogens, immunization, and infection protocols
CFA, HEL, and chicken OVA were purchased from Sigma-Aldrich. For regular CFA immunization, 20 µl of an emulsion of PBS and CFA (1:1) was intradermally injected either in the ear pinna or
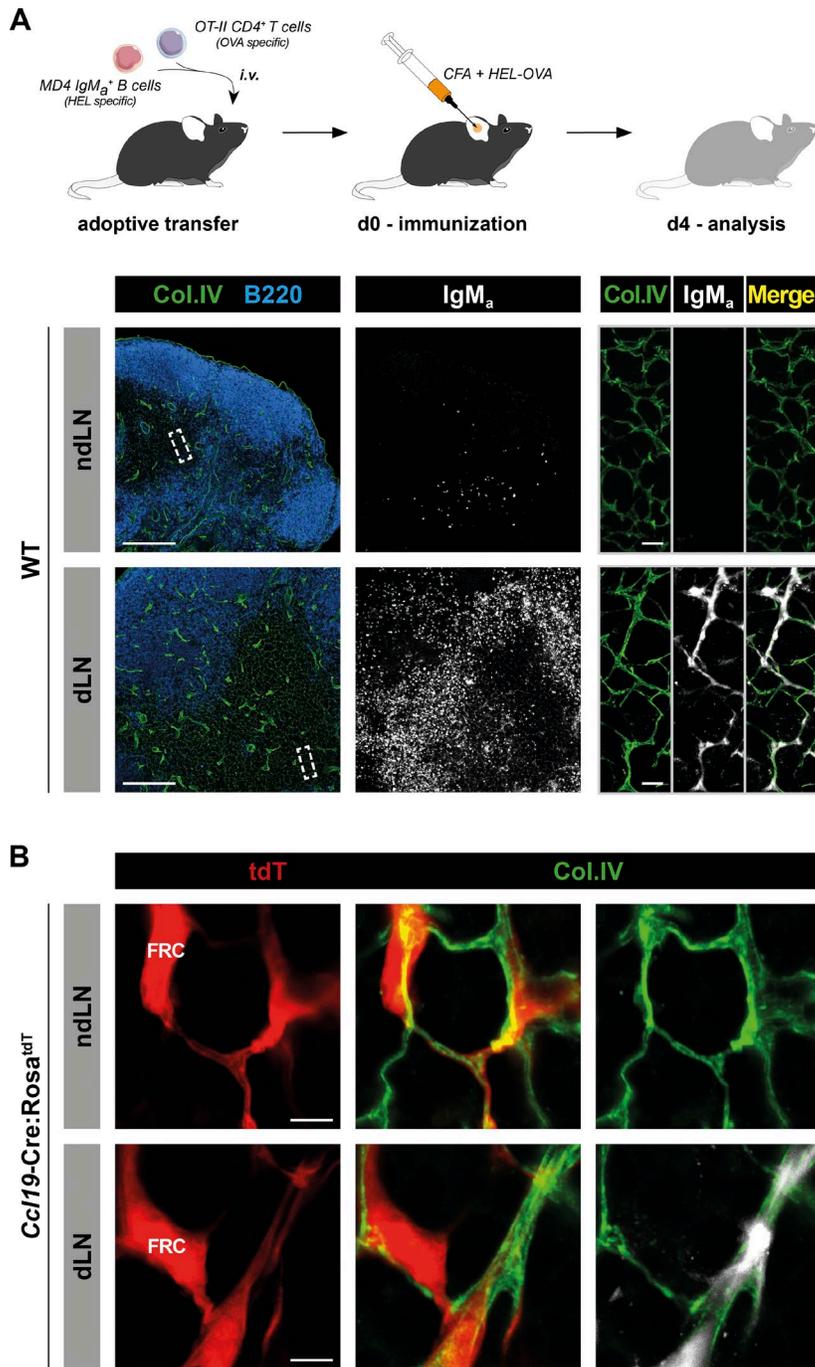
Figure 4. **Locally produced, Ag-specific IgM localizes within the conduit system of reactive LNs. (A)** HEL-specific MD4 IgM$_a$+ B cells and OVA-specific OT-II CD4+ T cells were adoptively transferred into WT mice. The next day, recipient mice were injected intradermally with an HEL-OVA chimeric protein emulsified in CFA, in one ear. 4 d later, auricular dLNs and contralateral ndLNs were harvested. Sections were stained for collagen IV (Col.IV), B220, and IgM$_a$ and imaged by confocal microscopy. tdT, tdTomato. Bars, 200 µm (left panels); 10 µm (right panels). Data are representative of three experiments (two mice per experiment). **(B)** Confocal imaging of reactive and contralateral LNs from *Ccl19*-Cre:Rosa[tdT] recipient mice treated as described in A. Bars, 5 µm. Data are representative of two experiments (two mice per experiment).

at the base of the tail of anesthetized mice. Draining auricular or inguinal LNs were harvested at the indicated time points. For immunization with an emulsion of CFA containing HEL-OVA chimeric protein, equimolar amounts of HEL and chicken OVA protein were combined in 0.0235% glutaraldehyde solution in phosphate buffer (pH 7.5) for 1 h at room temperature. After dialysis against PBS, the coupling product was filter-sterilized (0.2 µm) and stored at 4°C. Mice were intradermally injected in the ear pinna with 20 µl of an emulsion of PBS and CFA (1:1) containing 130 µg HEL-OVA conjugate. dLNs and contralateral ndLNs were harvested at the indicated time points. For VSV infection, mice were infected s.c. with 10[5] PFUs of VSV serotype Indiana dissolved in 10 µl PBS. Draining and nondraining popliteal or auricular LNs were collected at the indicated time points after in-
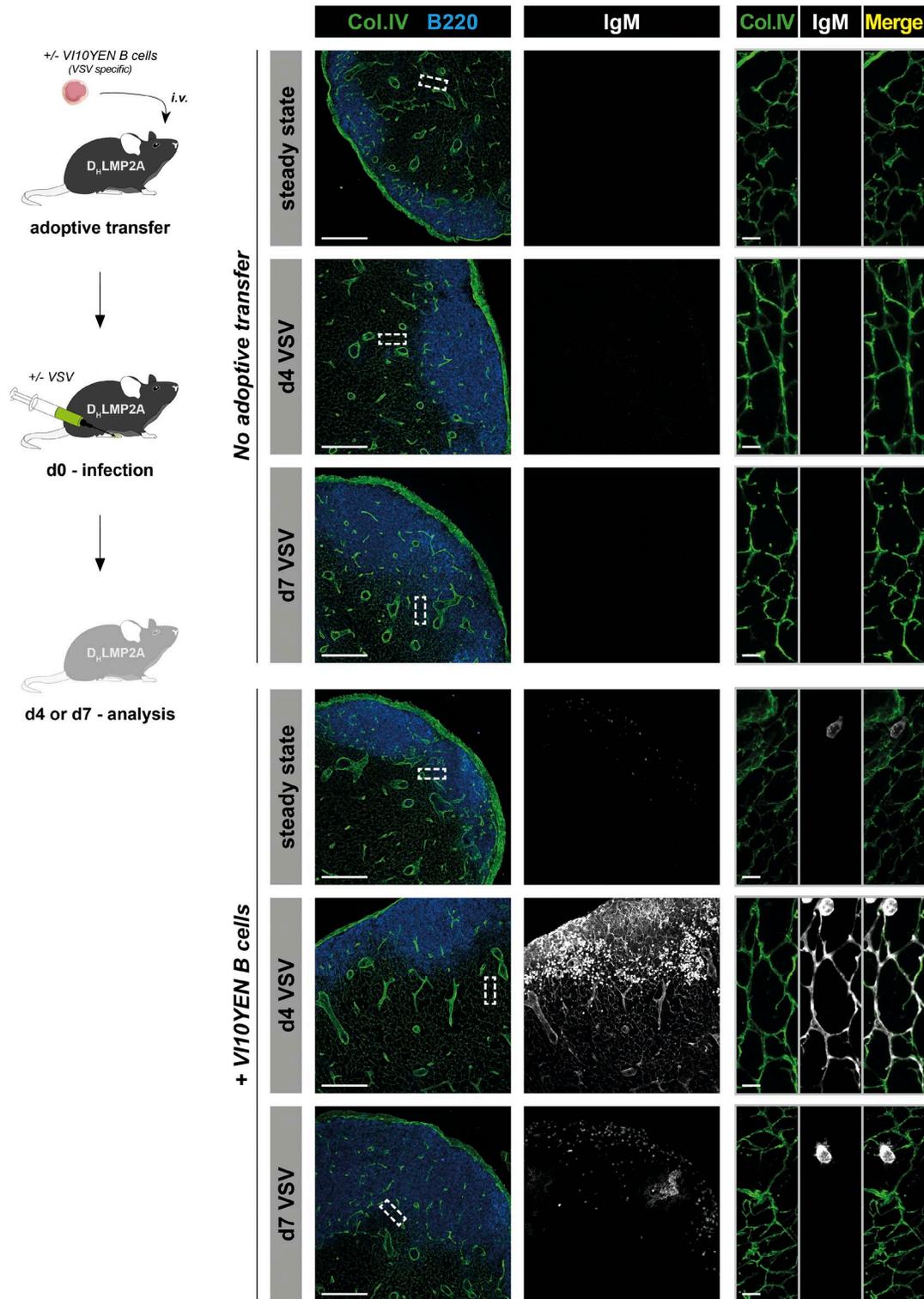
Figure 5.   **Antiviral IgM localizes within the conduit system of reactive LNs.** VSV-specific VI10YEN B cells were adoptively transferred in antibody-deficient D_HLMP2A mice. Recipients were either infected s.c. with VSV in the footpad or left untreated. 4 and 7 d later, reactive (popliteal) and steady state LNs were harvested. Mice that were not adoptively transferred with B cells served as controls. Sections were stained for collagen IV, B220, and IgM and analyzed by confocal microscopy. Insets show high-magnification views of conduits from the T cell zone. Bars, 200 µm (left panels); 10 µm (right panels). Data are representative of two experiments (at least one individual per condition and experiment).

fection for confocal imaging. All infectious work was performed in designated biosafety level (BSL)-2 and BSL-3 workspaces in accordance with institutional guidelines.

Subcutaneous tracer injections
20 µl PBS containing 10 µg fluorescent WGA ± 10 µg purified IgM was injected in the ear pinna of unimmunized mice or an-

imals that received an intradermal injection of CFA 10 d before. dLNs and contralateral ndLNs were harvested at the indicated time points following injection. In experiments involving soluble dextran, 20 µl PBS containing 150 or 100 µg fluorescent dextran weighing 10 kD and 150 kD, respectively, was injected.

Intranodal injections

Mice were immunized with an emulsion of CFA at the base of the tail. 10 d later, animals were anesthetized using a combination of ketamine and xylazine. Reactive inguinal LNs were exposed, and 1 µl PBS containing 0.3 µg fluorescent WGA ± purified IgM (0.3 µg; Figs. 3 A and S2 A) or fluorescent IgM (0.6 µg; Fig. 2, C and D) was injected into LNs with a 2.5-µl Hamilton syringe mounted with a 33G needle. In experiments involving fluorescent 150-kD dextran, 0.5 µl PBS containing 1.25 µg soluble dextran was injected. Reactive LNs were harvested 5 min following injection.

Transfer of immune sera

WT and J$_H$T mice were immunized with an intradermal injection of CFA in the ear pinna. On day 10, WT mice were sacrificed, and the blood was pooled and allowed to clot. Serum was then collected by centrifugation at 10,000 g for 6 min. J$_H$T mice were supplemented with 1 ml WT immune sera in multiple i.v. injections over a 24-h period. Serum and 200 µg fluorescent WGA were coadministered for the last injection, 5 min before the harvest of reactive and contralateral LNs.

Adoptive transfer experiments

For HEL-OVA immunization, LNs and spleens from OT-II and MD4 mice were minced with scissors and digested for 30 min at 37°C in RPMI medium containing 0.1 mg/ml DNase I (Sigma) and 1 mg/ml liberase (Roche). OT-II T cells and MD4 B cells were purified by negative selection using, respectively, CD11b/CD8/B220 and CD11b/CD3 biotin-conjugated antibodies followed by anti-biotin microbeads (Miltenyi Biotec). Ten million purified OT-II T cells and 3×10^7 MD4 B cells were injected i.v. in recipient mice 24 h before immunization with an emulsion of CFA containing HEL-OVA chimeric protein. For VSV infection, naive B cells from spleens of VI10YEN mice were negatively selected by magnetic isolation with CD43 beads (Miltenyi Biotec). The purity was ∼98% as determined by B220 staining. Five million B cells were injected i.v. into the indicated recipient animals 18 h before virus infection.

Tamoxifen treatment of *Prox1*-CreER^{T2}:Rosa^{tdT} mice

Mice were orally treated with 200 µl corn oil containing 5 mg tamoxifen (Sigma-Aldrich) 1 wk before immunization with CFA.

Immunostaining and confocal microscopy

LNs were fixed in AntigenFix (Microm Microtech) for 2 h at 4°C in the dark, washed in phosphate buffer, and dehydrated in 30% sucrose in 0.1 M phosphate buffer for 12 h. Samples were embedded in Tissue Freezing Medium (Triangle Biomedical Sciences), snap frozen, and sectioned (35 µm) on a cryostat (Leica Microsystems). Immunostaining was realized in 0.1 M UltraPure Tris Buffer (Thermo Fisher Scientific) containing 0.5% BSA and 1% Triton X-100. Confocal imaging was performed with a Zeiss LSM 880 confocal microscope. Separate images were collected for each fluorochrome and overlaid to obtain a multicolor image. Final image processing and 3D reconstruction were performed with Imaris software (Bitplane). For unfixed LN slice preparation, fresh LNs were embedded in 4% low-melting-temperature agarose (type VII-A; Sigma-Aldrich), sectioned in 300-µm-thick slices using a vibratome (Leica VT1200) in a bath of ice-cold PBS, and immediately imaged by confocal microscopy.

EM

LNs were fixed in AntigenFix for 2 h at 4°C and washed in 0.1 M phosphate buffer for 30 min. Samples were embedded in 4% agarose and sliced with a vibratome (Leica VT1200). 200-µm-thick sections were blocked for 30 min in 0.1 M UltraPure Tris Buffer containing 5% BSA and 5% goat serum (Jackson ImmunoResearch). Immunolabeling for mouse IgM was performed during 2 h. Sections were then washed in PBS and postfixed in PBS containing 2% PFA and 2.5% glutaraldehyde at 4°C overnight. The next day, samples were postfixed in aqueous 1% OsO$_4$ for 1 h and incubated overnight in aqueous 1% uranyl acetate. 1 d later, sections were dehydrated in graded series of ethanol baths (10 min each) and infiltrated with epon resin in ethanol (1:3, 2:2, 3:1, 2 h each and pure resin overnight). They were then embedded in fresh pure epon resin and cured for 48 h at 60°C. 70-nm ultrathin sections were performed on a Leica UCT Ultramicrotome and deposited on formvar-coated slot grids. The grids were contrasted using lead citrate and observed in an FEI Tecnai G2 at 200 kV. Imaging was performed on a Veleta camera (Olympus). Image processing and conduit area measurement were performed in ImageJ (National Institutes of Health).

Transport rate within the conduit system

To assess the transport rate of soluble material within the conduits, 5 µl PBS containing 5 µg fluorescent AF555-WGA was injected in the ear pinna of WT mice that received an intradermal injection of CFA 4 d before. Draining reactive auricular LNs from anesthetized mice were surgically exposed and harvested at the indicated time. The distance between the SCS and the migration front of WGA was calculated using ImageJ, while the percentage of the conduit system filled with WGA (from the SCS to 400 µm below) was calculated using the skeleton (3D) plugin of ImageJ. In brief, for each picture, we summed the total length of WGA-filled collagen IV fibers and divided it by the total length of collagen IV fibers.

Statistical analysis

Results are expressed as mean ± SEM. All statistical analyses were performed in Prism 7 (GraphPad Software). Groups were compared two-by-two using nonparametric two-tailed Mann–Whitney test.

Online supplemental material

Fig. S1 shows lymph- and blood-borne tracer dispersal in LNs from J$_H$T and D$_H$LMP2A mice. Fig. S2 demonstrates the ability of the conduit system to transport soluble IgM and large molecules upon intranodal injection in reactive LNs. Fig. S3 highlights the connectivity between the conduit system and the cortical and medullary sinusoids.

Acknowledgments

References

Adair, T.H., and A.C. Guyton. 1983. Modification of lymph by lymph nodes. II. Effect of increased lymph node venous blood pressure. *Am. J. Physiol.* 245:H616–H622.

Ager, A. 2017. High Endothelial Venules and Other Blood Vessels: Critical Regulators of Lymphoid Organ Development and Function. *Front. Immunol.* 8:45. https://doi.org/10.3389/fimmu.2017.00045

Anderson, A.O., and N.D. Anderson. 1975. Studies on the structure and permeability of the microvasculature in normal rat lymph nodes. *Am. J. Pathol.* 80:387–418.

Bajénoff, M. 2012. Stromal cells control soluble material and cellular transport in lymph nodes. *Front. Immunol.* 3:304. https://doi.org/10.3389/fimmu.2012.00304

Barnden, M.J., J. Allison, W.R. Heath, and F.R. Carbone. 1998. Defective TCR expression in transgenic mice constructed using cDNA-based alpha- and beta-chain genes under the control of heterologous regulatory elements. *Immunol. Cell Biol.* 76:34–40. https://doi.org/10.1046/j.1440-1711.1998.00709.x

Baumgarth, N., O.C. Herman, G.C. Jager, L.E. Brown, L.A. Herzenberg, and J. Chen. 2000. B-1 and B-2 cell-derived immunoglobulin M antibodies are nonredundant components of the protective response to influenza virus infection. *J. Exp. Med.* 192:271–280. https://doi.org/10.1084/jem.192.2.271

Bazigou, E., O.T. Lyons, A. Smith, G.E. Venn, C. Cope, N.A. Brown, and T. Makinen. 2011. Genes regulating lymphangiogenesis control venous valve formation and maintenance in mice. *J. Clin. Invest.* 121:2984–2992. https://doi.org/10.1172/JCI58050

Cahill, R., J.B. Hay, H. Frost, and Z. Trnka. 1974. Changes in lymphocyte circulation after administration of antigen. *Haematologia (Budap.).* 8:321–334.

Carrasco, Y.R., and F.D. Batista. 2007. B cells acquire particulate antigen in a macrophage-rich area at the boundary between the follicle and the subcapsular sinus of the lymph node. *Immunity.* 27:160–171. https://doi.org/10.1016/j.immuni.2007.06.007

Casola, S., K.L. Otipoby, M. Alimzhanov, S. Humme, N. Uyttersprot, J.L. Kutok, M.C. Carroll, and K. Rajewsky. 2004. B cell receptor signal strength determines B cell fate. *Nat. Immunol.* 5:317–327. https://doi.org/10.1038/ni1036

Chai, Q., L. Onder, E. Scandella, C. Gil-Cruz, C. Perez-Shibayama, J. Cupovic, R. Danuser, T. Sparwasser, S.A. Luther, V. Thiel, et al. 2013. Maturation of lymph node fibroblastic reticular cells from myofibroblastic precursors is critical for antiviral immunity. *Immunity.* 38:1013–1024. https://doi.org/10.1016/j.immuni.2013.03.012

Couper, K.N., R.S. Phillips, F. Brombacher, and J. Alexander. 2005. Parasite-specific IgM plays a significant role in the protective immune response to asexual erythrocytic stage Plasmodium chabaudi AS infection. *Parasite Immunol.* 27:171–180. https://doi.org/10.1111/j.1365-3024.2005.00760.x

Diamond, M.S., E.M. Sitati, L.D. Friend, S. Higgs, B. Shrestha, and M. Engle. 2003. A critical role for induced IgM in the protection against West Nile virus infection. *J. Exp. Med.* 198:1853–1862. https://doi.org/10.1084/jem.20031223

Fooksman, D.R., T.A. Schwickert, G.D. Victora, M.L. Dustin, M.C. Nussenzweig, and D. Skokos. 2010. Development and migration of plasma cells in the mouse lymph node. *Immunity.* 33:118–127. https://doi.org/10.1016/j.immuni.2010.06.015

Garside, P., E. Ingulli, R.R. Merica, J.G. Johnson, R.J. Noelle, and M.K. Jenkins. 1998. Visualization of specific B and T lymphocyte interactions in the lymph node. *Science.* 281:96–99. https://doi.org/10.1126/science.281.5373.96

Gohin, I., M. Olivier, I. Lantier, M. Pépin, and F. Lantier. 1997. Analysis of the immune response in sheep efferent lymph during Salmonella abortusovis infection. *Vet. Immunol. Immunopathol.* 60:111–130. https://doi.org/10.1016/S0165-2427(97)00090-1

Goodnow, C.C.J., J. Crosbie, S. Adelstein, T.B. Lavoie, S.J. Smith-Gill, R.A. Brink, H. Pritchard-Briscoe, J.S. Wotherspoon, R.H. Loblay, K. Raphael, et al. 1988. Altered immunoglobulin expression and functional silencing of self-reactive B lymphocytes in transgenic mice. *Nature.* 334:676–682. https://doi.org/10.1038/334676a0

Gretz, J.E., E.P. Kaldjian, A.O. Anderson, and S. Shaw. 1996. Sophisticated strategies for information encounter in the lymph node: the reticular network as a conduit of soluble information and a highway for cell traffic. *J. Immunol.* 157:495–499.

Gretz, J.E., A.O. Anderson, and S. Shaw. 1997. Cords, channels, corridors and conduits: critical architectural elements facilitating cell interactions in the lymph node cortex. *Immunol. Rev.* 156:11–24. https://doi.org/10.1111/j.1600-065X.1997.tb00955.x

Gretz, J.E., C.C. Norbury, A.O. Anderson, A.E. Proudfoot, and S. Shaw. 2000. Lymph-borne chemokines and other low molecular weight molecules reach high endothelial venules via specialized conduits while a functional barrier limits access to the lymphocyte microenvironments in lymph node cortex. *J. Exp. Med.* 192:1425–1440. https://doi.org/10.1084/jem.192.10.1425

Gu, H., Y.R. Zou, and K. Rajewsky. 1993. Independent control of immunoglobulin switch recombination at individual switch regions evidenced through Cre-loxP-mediated gene targeting. *Cell.* 73:1155–1164. https://doi.org/10.1016/0092-8674(93)90644-6

Haig, D.M., J. Hopkins, and H.R. Miller. 1999. Local immune responses in afferent and efferent lymph. *Immunology.* 96:155–163. https://doi.org/10.1046/j.1365-2567.1999.00681.x

Hangartner, L., B.M. Senn, B. Ledermann, U. Kalinke, P. Seiler, E. Bucher, R.M. Zellweger, K. Fink, B. Odermatt, K. Bürki, et al. 2003. Antiviral immune responses in gene-targeted mice expressing the immunoglobulin heavy chain of virus-neutralizing antibodies. *Proc. Natl. Acad. Sci. USA.* 100:12883–12888. https://doi.org/10.1073/pnas.2135542100

Hayakawa, M., M. Kobayashi, and T. Hoshino. 1988. Direct contact between reticular fibers and migratory cells in the paracortex of mouse lymph nodes: a morphological and quantitative study. *Arch. Histol. Cytol.* 51:233–240. https://doi.org/10.1679/aohc.51.233

Huang, H.Y., A. Rivas-Caicedo, F. Renevey, H. Cannelle, E. Peranzoni, L. Scarpellino, D.L. Hardie, A. Pommier, K. Schaeuble, S. Favre, et al. 2018. Identification of a new subset of lymph node stromal cells involved in regulating plasma cell homeostasis. *Proc. Natl. Acad. Sci. USA.* 115:E6826–E6835. https://doi.org/10.1073/pnas.1712628115

Jafarnejad, M., M.C. Woodruff, D.C. Zawieja, M.C. Carroll, and J.E. Moore Jr. 2015. Modeling Lymph Flow and Fluid Exchange with Blood Vessels in

Lymph Nodes. *Lymphat. Res. Biol.* 13:234–247. https://doi.org/10.1089/lrb.2015.0028

Junt, T., E.A. Moseman, M. Iannacone, S. Massberg, P.A. Lang, M. Boes, K. Fink, S.E. Henrickson, D.M. Shayakhmetov, N.C. Di Paolo, et al. 2007. Subcapsular sinus macrophages in lymph nodes clear lymph-borne viruses and present them to antiviral B cells. *Nature.* 450:110–114. https://doi.org/10.1038/nature06287

Kalinke, U., A. Krebber, C. Krebber, E. Bucher, A. Plückthun, R.M. Zinkernagel, and H. Hengartner. 1996. Monovalent single-chain Fv fragments and bivalent miniantibodies bound to vesicular stomatitis virus protect against lethal infection. *Eur. J. Immunol.* 26:2801–2806. https://doi.org/10.1002/eji.1830261202

Luther, S.A., A. Gulbranson-Judge, H. Acha-Orbea, and I.C. MacLennan. 1997a. Viral superantigen drives extrafollicular and follicular B cell differentiation leading to virus-specific antibody production. *J. Exp. Med.* 185:551–562. https://doi.org/10.1084/jem.185.3.551

Luther, S.A., I. Maillard, F. Luthi, L. Scarpellino, H. Diggelmann, and H. Acha-Orbea. 1997b. Early neutralizing antibody response against mouse mammary tumor virus: critical role of viral infection and superantigen-reactive T cells. *J. Immunol.* 159:2807–2814.

Lutz, C., B. Ledermann, M.H. Kosco-Vilbois, A.F. Ochsenbein, R.M. Zinkernagel, G. Köhler, and F. Brombacher. 1998. IgD can largely substitute for loss of IgM function in B cells. *Nature.* 393:797–801. https://doi.org/10.1038/31716

MacLennan, I.C., K.M. Toellner, A.F. Cunningham, K. Serre, D.M. Sze, E. Zúñiga, M.C. Cook, and C.G. Vinuesa. 2003. Extrafollicular antibody responses. *Immunol. Rev.* 194:8–18. https://doi.org/10.1034/j.1600-065X.2003.00058.x

Madisen, L., T.A. Zwingman, S.M. Sunkin, S.W. Oh, H.A. Zariwala, H. Gu, L.L. Ng, R.D. Palmiter, M.J. Hawrylycz, A.R. Jones, et al. 2010. A robust and high-throughput Cre reporting and characterization system for the whole mouse brain. *Nat. Neurosci.* 13:133–140. https://doi.org/10.1038/nn.2467

Mondor, I., A. Jorquera, C. Sene, S. Adriouch, R.H. Adams, B. Zhou, S. Wienert, F. Klauschen, and M. Bajénoff. 2016. Clonal Proliferation and Stochastic Pruning Orchestrate Lymph Node Vasculature Remodeling. *Immunity.* 45:877–888. https://doi.org/10.1016/j.immuni.2016.09.017

Moseman, E.A., M. Iannacone, L. Bosurgi, E. Tonti, N. Chevrier, A. Tumanov, Y.X. Fu, N. Hacohen, and U.H. von Andrian. 2012. B cell maintenance of subcapsular sinus macrophages protects against a fatal viral infection independent of adaptive immunity. *Immunity.* 36:415–426. https://doi.org/10.1016/j.immuni.2012.01.013

Ochsenbein, A.F., D.D. Pinschewer, B. Odermatt, M.C. Carroll, H. Hengartner, and R.M. Zinkernagel. 1999. Protective T cell-independent antiviral antibody responses are dependent on complement. *J. Exp. Med.* 190:1165–1174. https://doi.org/10.1084/jem.190.8.1165

Ochsenbein, A.F., D.D. Pinschewer, S. Sierro, E. Horvath, H. Hengartner, and R.M. Zinkernagel. 2000. Protective long-term antibody memory by antigen-driven and T help-dependent differentiation of long-lived memory B cells to short-lived plasma cells independent of secondary lymphoid organs. *Proc. Natl. Acad. Sci. USA.* 97:13263–13268. https://doi.org/10.1073/pnas.230417497

Ono, S., G. Egawa, and K. Kabashima. 2017. Regulation of blood vascular permeability in the skin. *Inflamm. Regen.* 37:11. https://doi.org/10.1186/s41232-017-0042-9

Phan, T.G., I. Grigorova, T. Okada, and J.G. Cyster. 2007. Subcapsular encounter and complement-dependent transport of immune complexes by lymph node B cells. *Nat. Immunol.* 8:992–1000. https://doi.org/10.1038/ni1494

Phan, T.G., J.A. Green, E.E. Gray, Y. Xu, and J.G. Cyster. 2009. Immune complex relay by subcapsular sinus macrophages and noncognate B cells drives antibody affinity maturation. *Nat. Immunol.* 10:786–793. https://doi.org/10.1038/ni.1745

Racine, R., and G.M. Winslow. 2009. IgM in microbial infections: taken for granted? *Immunol. Lett.* 125:79–85. https://doi.org/10.1016/j.imlet.2009.06.003

Rantakari, P., K. Auvinen, N. Jäppinen, M. Kapraali, J. Valtonen, M. Karikoski, H. Gerke, I. Iftakhar-E-Khuda, J. Keuschnigg, E. Umemoto, et al. 2015. The endothelial protein PLVAP in lymphatics controls the entry of lymphocytes and antigens into lymph nodes. *Nat. Immunol.* 16:386–396. https://doi.org/10.1038/ni.3101

Roozendaal, R., T.R. Mempel, L.A. Pitcher, S.F. Gonzalez, A. Verschoor, R.E. Mebius, U.H. von Andrian, and M.C. Carroll. 2009. Conduits mediate transport of low-molecular-weight antigen to lymph node follicles. *Immunity.* 30:264–276. https://doi.org/10.1016/j.immuni.2008.12.014

Sainte-Marie, G., and F.S. Peng. 1986. Diffusion of a lymph-carried antigen in the fiber network of the lymph node of the rat. *Cell Tissue Res.* 245:481–486. https://doi.org/10.1007/BF00218547

Salinas-Carmona, M.C., and I. Pérez-Rivera. 2004. Humoral immunity through immunoglobulin M protects mice from an experimental actinomycetoma infection by Nocardia brasiliensis. *Infect. Immun.* 72:5597–5604. https://doi.org/10.1128/IAI.72.10.5597-5604.2004

Sixt, M., N. Kanazawa, M. Selg, T. Samson, G. Roos, D.P. Reinhardt, R. Pabst, M.B. Lutz, and L. Sorokin. 2005. The conduit system transports soluble antigens from the afferent lymph to resident dendritic cells in the T cell area of the lymph node. *Immunity.* 22:19–29. https://doi.org/10.1016/j.immuni.2004.11.013

Soderberg, K.A., G.W. Payne, A. Sato, R. Medzhitov, S.S. Segal, and A. Iwasaki. 2005. Innate control of adaptive immunity via remodeling of lymph node feed arteriole. *Proc. Natl. Acad. Sci. USA.* 102:16315–16320. https://doi.org/10.1073/pnas.0506190102

Ushiki, T., O. Ohtani, and K. Abe. 1995. Scanning electron microscopic studies of reticular framework in the rat mesenteric lymph node. *Anat. Rec.* 241:113–122. https://doi.org/10.1002/ar.1092410115